http://dx.doi.org/10.5607/en.2013.22.4.283
Exp Neurobiol. 2013 Dec;22(4):283-300.
pISSN 1226-2560 • eISSN 2093-8144

Original Article

Experimental Neurobiology

Mitochondrial Dysfunction of Immortalized Human Adipose Tissue-Derived Mesenchymal Stromal Cells from Patients with Parkinson's Disease

Hyo Eun Moon[1,2,3], Seung Hee Yoon[5], Yong Suk Hur[6], Hyung Woo Park[1,2,3], Ji Young Ha[5], Kyung-Hee Kim[5], Jung Hee Shim[5], Seung Hyun Yoo[6], Jin H. Son[5], Seung Leal Paek[1,2,3,8], In Keyoung Kim[1], Jae Ha Hwang[1], Dong Gyu Kim[1], Han-Joon Kim[4], Beom Seok Jeon[4], Sung Sup Park[7] and Sun Ha Paek[1,2,3]*

[1]Department of Neurosurgery, [2]Cancer Research Institute, [3]Ischemic/Hypoxic Disease Institute, Seoul National University College of Medicine, [4]Department of Neurology, Seoul National University College of Medicine, Seoul 110-744, [5]Department of Brain & Cognitive Sciences, College of Pharmacy, Brain Disease Research Institute, Ewha Woman's University, Seoul 120-750, [6]Department of Biochemistry, Inha University School of Medicine, Incheon 402-751, [7]Department of Laboratory Medicine, Seoul National University Hospital, Seoul 110-744, Korea, [8]Department of Neurosurgery, Mayo Clinic, USA

Mitochondrial dysfunction in dopaminergic neurons of patients with idiopathic and familial Parkinson's disease (PD) is well known although the underlying mechanism is not clear. We established a homogeneous population of human adipose tissue-derived mesenchymal stromal cells (hAD-MSCs) from human adult patients with early-onset hereditary familial Parkin-defect PD as well as late-onset idiopathic PD by immortalizing cells with the hTERT gene to better understand the underlying mechanism of PD. The hAD-MSCs from patients with idiopathic PD were designated as "*PD*", from patients with Parkin-defect PD as "*Parkin*" and from patients with pituitary adenomas as "*non-PD*" in short. The pGRN145 plasmid containing hTERT was introduced to establish telomerase immortalized cells. The established hTERT-immortalized cell lines showed chromosomal aneuploidy sustained stably over two-years. The morphological study of mitochondria in the primary and immortalized hAD-MSCs showed that the mitochondria of the *non-PD* were normal; however, those of the *PD* and *Parkin* were gradually damaged. A striking decrease in mitochondrial complex I, II, and IV activities was observed in the hTERT-immortalized cells from the patients with idiopathic and Parkin-defect PD. Comparative Western blot analyses were performed to investigate the expressions of PD specific marker proteins in the hTERT-immortalized cell lines. This study suggests that the hTERT-immortalized hAD-MSC cell lines established from patients with idiopathic and familial Parkin-defect PD could be good cellular models to evaluate mitochondrial dysfunction to better understand the pathogenesis of PD and to develop early diagnostic markers and effective therapy targets for the treatment of PD.

Key words: hTERT, hAD-MSC, immortalization, Parkinson's disease, diagnosis

Received November 12, 2013, Revised November 22, 2013, Accepted November 22, 2013

* To whom correspondence should be addressed.
TEL: 82-2-2072-3993, FAX: 82-2-744-8459
e-mail: paeksh@snu.ac.kr

INTRODUCTION

Parkinson's disease (PD) is characterized by the selective loss of dopaminergic (DA) neurons in the substantia nigra pars compacta (SNpc) as well as by complex interactions between susceptible genes and various environmental risk factors [1-3]. Aberrant mitochondrial forms and functions are widely accepted pathogenic mechanisms in a subset of people with PD [2, 3]. Mitochondrial dysfunction in the dopaminergic neurons of idiopathic and familial PD is well known although the underlying mechanisms are not clear. The most direct evidence for disrupted mitochondrial metabolism has come from studies using autopsy tissues and other tissue samples and from *in vitro* cell cultures derived from human patients with PD [2]. Moreover, mitochondrial abnormalities have been reported in Parkin-defect mouse and fruit fly models of PD [4-6]. For instance, oxidative damage, Lewy body formation and decreased mitochondrial complex I activity are consistent pathological findings in PD [7]. Impaired mitochondrial function leads to increased oxidative stress (OS) and OS has a significant pathogenic role in the selective loss of DA neurons in human patients [8] and in experimental models for PD [9]. OS or reactive oxygen species (ROS) not only implicit direct cellular damages but also activate signaling pathways leading to cell death [10]. Apoptosis contributes to DA neuronal loss in the SNpc of PD patients as well as in neurotoxin models [11, 12]. Autophagy has been suggested as an alternative mechanism of cell death in neurotoxin models [13], in the familial PD gene mutant model [14] and in human PD brains [15]. Mitochondria have an important role in pro-inflammatory signaling. Autophagic turnover of cellular constituents eliminates dysfunctional or damaged mitochondria thus counteracting degeneration and inflammation and preventing unwarranted cell loss. Decreased expression of genes that regulate autophagy can cause neurodegenerative diseases in which deficient quality control results in inflammation and in the death of neuronal cell populations. One feature of the mammalian target of rapamycin (mTOR) kinase inhibition is autophagy. Thus, a combination of mitochondrial dysfunction and insufficient autophagy may contribute to PD pathogenesis [16].

Multipotent mesenchymal stromal cells (MSC) from human adipose tissue represent an excellent source of progenitor cells for cell therapy and tissue engineering [17, 18]. Human adipose tissue is a rich source of MSC providing an abundant and accessible source of adult stem cells. Here, we isolated human adipose tissue-derived mesenchymal stromal cells (hAD-MSCs) from patients with idiopathic PD designated as "*PD*," from patients with Parkin-defect PD as "*Parkin*" and from patients with non-PD pituitary adenomas as "*non-PD*" in short.

In culture, normal human cells have a finite lifespan ultimately ceasing to proliferate in a process called replicative senescence [19]. Telomeres are specific structures found at the ends of chromosomes in eukaryotes, which protect the chromosome ends [20]. Telomerase is a ribonucleoprotein that synthesizes and directs the telomeric repeats onto the 3' end of existing telomeres using its RNA component as a template [21]. Human telomerase reverse transcriptase (hTERT) is the catalytic component of a functional telomerase complex, which is important in maintaining cell immortality. In humans, telomere shortening limits the proliferative potential of somatic cells, and the introduction of hTERT is a valuable method that circumvents the attenuated mitotic competence of somatic cells associated with TERT inactivation [22].

In the present study, for the first time, to overcome the cellular senescence of primary cultured AD-MSCs from PD patients, we established hTERT-immortalized wild type, idiopathic and Parkin-defect mesenchymal stromal cell lines isolated from the adipose tissues of PD patients. Then, we used these immortalized cell lines to investigate mitochondrial abnormalities in the idiopathic and Parkin-defect PD cell lines compared to the wild type cell line. This study suggests that the hTERT-immortalized hAD-MSC cell lines established from patients with idiopathic and familial Parkin-defect PD could be good cellular models to evaluate mitochondrial dysfunction to better understand the pathogenesis of PD and to develop early diagnostic markers and effective therapy targets for the treatment of PD.

MATERIALS AND METHODS

Primary cultures of hAD-MSCs and collection of brain cortexes from PD patients

This study was approved by the institutional review board of the Biomedical Research Institute of Seoul National University Hospital (IRB No. 0707-024-212). Written informed consent was obtained from the patients. Subcutaneous adipose tissue was acquired during the Deep Brain Stimulation (DBS) surgery performed in patients with idiopathic and Parkin-defect PD and compared with non-PD patients with pituitary adenomas. The primary hAD-MSCs were obtained from the abdominal subcutaneous adipose tissues of two non-PD patients, which were a 48-year-old female and a 28-year-old male with pituitary adenomas, from the subclavicular subcutaneous adipose tissues of two idiopathic PD patients, which were a 65-year-old female and a 68-year-old male, and from the subclavicular subcutaneous adipose tissues of two Parkin-defect PD patients

http://dx.doi.org/10.5607/en.2013.22.4.283

which were a 26-year-old female and a 36-year-old female. The primary hAD-MSCs of the PD and non-PD patients were isolated from adipose tissues as previously described [23] and maintained in Mesenchymal Stem cell Expansion medium (Millipore, Billerica, MA, USA). The culture medium was replaced every 3 days. Phenotypical characterization and quantitative analyses of the putative hAD-MSCs were previously described [23]. Simultaneously, the brain cortex tissues of early onset and idiopathic PD patients were obtained from DBS surgery (IRB No. H-0812-046-266) and immediately frozen and stored at -80°C in a deep freezer while that of non-PD resected from patients was from normal brain tissue banking (IRB No. H-0805-036-243).

Immortalization of mesenchymal stromal cells derived from the adipose tissues of PD patients with pGRN145 that included hTERT

The day before transfection, cells were replated in a 24-well plate without antibiotics so that they would reach 90% confluence on the day of transfection. For each well, 50 μL of serum-free OPTI-MEM I Medium (Gibco BRL, Grand Island, NY, USA) containing 1 μg of pGRN145 plasmid (Geron Corporation, Menlo Park, USA) was combined with 50 μL of OPTI-MEM I Medium containing LIPOFECTAMINE LTX Reagent (Gibco BRL, Grand Island, NY, USA). The pGRN145 construct consisted of a mammalian expression vector containing the hTERT open reading frame minus the 5' and the 3' UTR under the control of the myeloproliferative sarcoma virus promoter (MPSV LTR). The mixture was then added to each well and the plate was gently shaken. After 24 h of incubation at 37°C, the culture medium was changed with fresh medium. After 48 h, the transfected cells were plated in medium containing Hygromycin-B in PBS (30 μg/mL, Invitrogen, Carlsbad, CA, USA) for two to three weeks. After treatment, cell death occurs rapidly allowing for the selection of transfected cells and single-cell derived clones were selected and expanded. After which, the concentration of Hygromycin-B was reduced to 10 μg/mL.

Telomeric Repeat Amplification Protocol (TRAP) assay

The telomerase activity was assayed with TRAP using the TRAPEZE® Telomerase Detection Kit (Chemicon International, Temecula, CA, USA). Cultured cells were solubilized in 200 μL of CHAPS lysis buffer (10 mM Tris-HCl pH 7.5, 1 mM $MgCl_2$, 1 mM EGTA, 0.1 mM Benzamidine, 5 mM β-mercaptoethanol, 0.5% CHAPS, 10% Glycerol). Five hundred nanograms of protein from each sample buffer were used in the TRAP assay. The assay mixture in TRAP buffer (20 mM Tris-HCl pH 8.3, 1.5 mM $MgCl_2$, 63 mM KCl, 0.05% Tween-20, 1 mM EGTA) contained the following: 50 μM dNTPs, 2 μg/mL TS primer, primer mix and 5 U/μL Tag polymerase (Promega). To test the specificity of the telomerase assay, 2 μL of cell extracts were pre-incubated at 85°C for 10 min and then added to heat inactivated control mixtures. Two microliters containing 500 cells of TSR8 (control template) were used as a positive control for telomerase activity. As negative controls, 2 μL of primary *non-PD*, *PD*, *Parkin* cells were used. All samples were first incubated at 30°C for 30 min to allow telomerase-mediated extension of the TS primer. The samples were then amplified by PCR (94°C/30 sec, 59°C/30 sec, 72°C/1 min, for 33 cycles, and 72°C/15 min). The products were resolved on a 10% non-denaturing PAGE gel in 0.5×TBE buffer.

Karyotyping analysis

To establish whether the immortalized lines were euploidy, the cells were subjected to metaphase mitotic arrest using Colcemid (Gibco) stock solution. After which, the cells were harvested by centrifugation at 1,500 rpm, subjected to hypotonic shock with 0.075 M KCl, and fixed by adding Carnoy's fixative (3:1 methanol:acetic acid) and Giemsa staining (GTG banding). Prepared cell slides were then analyzed with the Karyotype Analysis program ChIPS-Karyo (Chromosome Image Processing System) (GenDix, Inc. Seoul, Korea).

Separation of mitochondria from cultured cells for mitochondrial complex I, II, IV and citrate synthase assays

Isolation of mitochondria

The *non-PD*, *PD*, and *Parkin* cells immortalized with hTERT were washed with ice-cold phosphate buffered saline (PBS) and suspended in ice-cold 10 mM Tris that included a protease inhibitor cocktail (pH 7.6). We disrupted the cells mechanically with a 1 mL syringe, immediately added ice-cold 1.5 M sucrose and then centrifuged them at 600 g for 10 min at 2°C. The supernatant was centrifuged again at 14,000 g for 10 min at 2°C, and the resulting pellet was washed with ice-cold 10 mM Tris that included a protease inhibitor cocktail (pH 7.6). The mitochondrial pellet was resuspended in 10 mM Tris that included a protease inhibitor cocktail (pH 7.6), and the total protein content was quantified with the Bradford assay. The other samples were kept on ice until use.

Complex I assay

The activity was determined in isolated mitochondrial preparations. We measured complex I activity as described in [24] with some modifications. We measured complex I spectrophotometrically at 600 nm in an incubation volume of 240 μL containing 25 mM potassium phosphate, 3.5 g/L BSA, 60 μM

DCIP, 70 μM decylubiquinone, 1.0 μM antimycine-A and 3.2 mM NADH, pH 7.8. The obtained mitochondrial samples (1 μg/10 μL) were added to buffer without NADH. We preincubated the samples in the mixture for 3 min at 37°C. After adding 5 μL of 160 mM NADH, the absorbance was measured at 30-s intervals for 5 min at 37°C. After 5 min, we added 2.5 μL of rotenone (1 mM in dimethylsulfoxide and diluted to 100 μM in 10 mM Tris, pH 7.6) and measured the absorbance at 30-s intervals for 5 min at 37°C.

Complex II assay

The activity was determined in isolated mitochondrial preparations. We measured the complex II activity as described in [24] with some modifications. We measured the complex II activity spectrophotometrically at 600 nm in an incubation volume of 240 μL containing 80 mM potassium phosphate, 1 g/L BSA, 2 mM EDTA, 0.2 mM ATP, 10 mM succinate, 0.3 mM potassium cyanide, 60 μM DCIP, 50 μM decylubiquinone, 1 μM antimycine-A and 3 μM rotenone, pH 7.8. Specifically, the obtained mitochondrial samples (1 μg/10 μL) were added to buffer without succinate and potassium cyanide. We preincubated the samples in the mixture for 10 min at 37°C. After adding 20 μL of 1.5 M succinate and 0.75 μL of 0.1 M KCN, the absorbance was measured at 30-s intervals for 5 min at 37°C. Blanks were measured in the presence of 5 mM malonate that was added before preincubation.

Complex IV assay

The activity was determined in isolated mitochondrial preparations. We measured the complex IV activity as described in [25] with some modifications. We measured the complex IV activity spectrophotometrically at 550 nm in an incubation volume of 240 μL containing 30 mM potassium phosphate, 2.5 mM dodecylmaltoside and 34 μM ferrocytochrome c, pH 7.4. Specifically, the obtained mitochondrial samples (1 μg/10 μL) were added to the buffer and their absorbance was immediately measured at 30-s intervals for 5 min at 30°C. Blanks were measured in the presence of 1 mM KCN.

Citrate synthase assay

The activity was determined in isolated mitochondrial preparations. We measured the citrate synthase activity as described in [26] with some modifications. We measured the citrate synthase activity spectrophotometrically at 412 nm in an incubation volume of 240 μL containing 50 mM Tris-HCl, 0.2 mM 5,5'-dithiobis-(2-nitrobenzoic acid), 0.1 mM acetyl-CoA and 0.5 mM oxaloacetate, pH 7.5. Specifically, the obtained mitochondrial samples (1 μg/10 μL) were added to the buffer without oxaloacetate. We preincubated the samples in the mixture for 5 min at 30°C. After adding 2.5 μL of 50 mM oxaloacetate, the absorbance was measured at 30-s intervals for 5 min at 37°C. The assay was initiated by the addition of oxaloacetate, and an equivalent volume of water was added to the controls.

Western blot analysis

Cells were washed in cold PBS and lysed in lysis buffer (cell signaling) and PMSF at 4°C. The lysates were clarified by centrifugation to remove the insoluble components at 15,000 g for 20 min at 4°C. The protein content of the cell lysates were normalized with Bradford reagent (Bio-Rad). Equal amounts of proteins, which were the same amounts used for the immortalized cells, were loaded onto a SDS-PAGE gel, electrophoresed, transferred to a PVDF membrane (Millipore) and blocked with 5% non-fat dry milk in TBST. The immunoreactive proteins on the membrane were detected with chemiluminescence using the ECL-Plus substrate (GE Healthcare, Buckinghamshire, USA) on X-ray films. Antibodies for HSP60, HSP90, Cytochrome b5 and GRP78 were obtained from Santa Cruz Biotechnology (Santa Cruz, CA, USA). Prohibitin and β-actin (Santa Cruz) were used as internal controls. Western blot analysis was performed with the National Institutes of Health image processing and analyzing program (ImageJ, v1.38; http://rsb.info.nih.gov/ij/).

Electron microscopy

Cells grown on culture dishes were washed in PBS and fixed with 0.1% glutaraldehyde and 4% paraformaldehyde in PBS at 4°C for 2 h. The cells were collected and centrifuged at 2,000 g for 3 min at 4°C to obtain pellets. The prepared pellets were re-suspended in warm agar (1% in PBS) and centrifuged at 2,000 g for 3 min at 4°C to obtain the pellets again. Then, the pellets were washed with PBS three times, and the cell pellets embedded with agar were fixed again with 1% osmium tetroxide for 2 h and washed with PBS three times. The cell pellets embedded with agar were dehydrated with an ethanol series and fixed again with Epon 812. The ultrathin (70 nm) sections were collected on Formvar/carbon-coated nickel grids, and the grids were stained with 2.5% uranyl acetate for 7 min followed by lead citrate for 2.5 min, and then, the sections were observed with a JEOL JEM-1011 electron microscope.

Mitotracker staining

hAD-MSCs (1.5 x 10^4 cells) were seeded on gelatin-coated glass coverslips (NUNC, Rochester, USA). The next day, Mitotracker (Invitrogen, final 10 nM) in medium was added to the cells for 20 min at RT. The cells were washed with media and PBS and fixed with 4% PFA for 10 min at RT. After washing with PBS three times, the fluorescence was visualized with a confocal laser

http://dx.doi.org/10.5607/en.2013.22.4.283

scanning microscope (Carl Zeiss LSM 510META, Carl Zeiss, Jena, Germany).

Immunocytochemistry and confocal microscopy

The cells were fixed with 4% paraformaldehyde in PBS. After permeabilization with 0.3% Triton X-100 in PBS and blocking with 10% normal goat serum (NGS) in 0.1% BSA/PBS for 1 h, immunofluorescent staining was performed using the primary antibody anti-mitochondria (Millipore Corporation, Billerica, MA, USA). Subsequently, the cover glasses were incubated for 1 h at RT with a fluorescent-labeled secondary antibody anti-FITC (Alexa488-labeled, raised in mouse; Jackson ImmunoResearch Laboratories, West Grove, PA, USA) and mounted with Vectashield medium containing 4',6-diamidino-2-phenylindole (DAPI; Vector Laboratories Inc., Burlingame, CA, USA). The fluorescence was visualized using a confocal laser scanning microscope (Carl Zeiss LSM 510META, Carl Zeiss, Jena, Germany).

Immunofluorescence staining with frozen tissue

Human brain tissues in a nitrogen tank were thawed and placed for seven days in a 50 ml conical tube containing ice-cold 4% paraformaldehyde. The human brain tissues were then cut into 15-μm thick sections on a freezing cryostat (Leica CM3000, Leica, Solms, Germany). The brain sections were washed in distilled water followed by washing with PBS three times for five minutes each and permeabilized with PBS containing 0.05% (vol/vol) saponin and 5% (vol/vol) NGS for 15 min. Non-specific binding was blocked with 1.5% NGS for 15 min. This was followed by application of the mouse monoclonal anti-mitochondria antibody (Millipore Corporation, Billerica, MA, USA) incubated overnight at 4°C. After being washed three times in PBS for five minutes each, the sections were incubated with the fluorescent-labeled secondary antibodies Alexa 594 goat anti-mouse or rabbit IgG (1:500) for 1 h at RT followed by washing with PBS. The fluorescently labeled slices were analyzed on a Meta confocal microscope (LSM 510; Carl Zeiss MicroImaging, Inc., Jena, Germany) equipped with four lasers.

Statistical analysis

Statistical analysis was performed with GraphPad Prism v. 5.0 (GraphPad Software, San Diego, CA, USA). Summary data

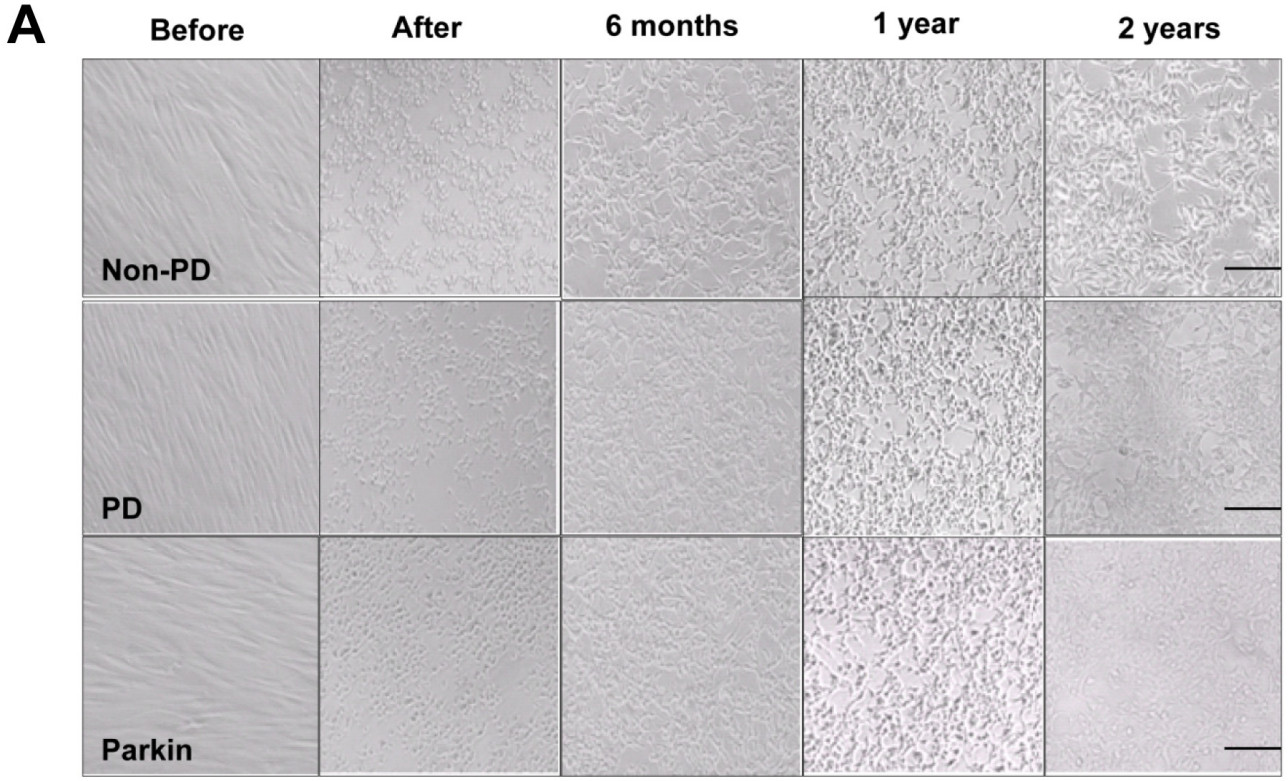

Fig. 1. Transduction of hTERT telomerase activity resulting in immortalized hAD-MSCs. (A) Morphology of pre- and post-immortal hAD-MSCs. *non-PD* showing the shape of the cells before and after immortalization, and in the 6-month, 1-year and 2-year cultures; *PD* showing the shape of the cells before and after immortalization, and in the 6-month, 1-year and 2-year cultures; *Parkin* showing the shape of cells before and after immortalization, and in the 6-month, 1-year and 2-year cultures. Bar=200 μm.

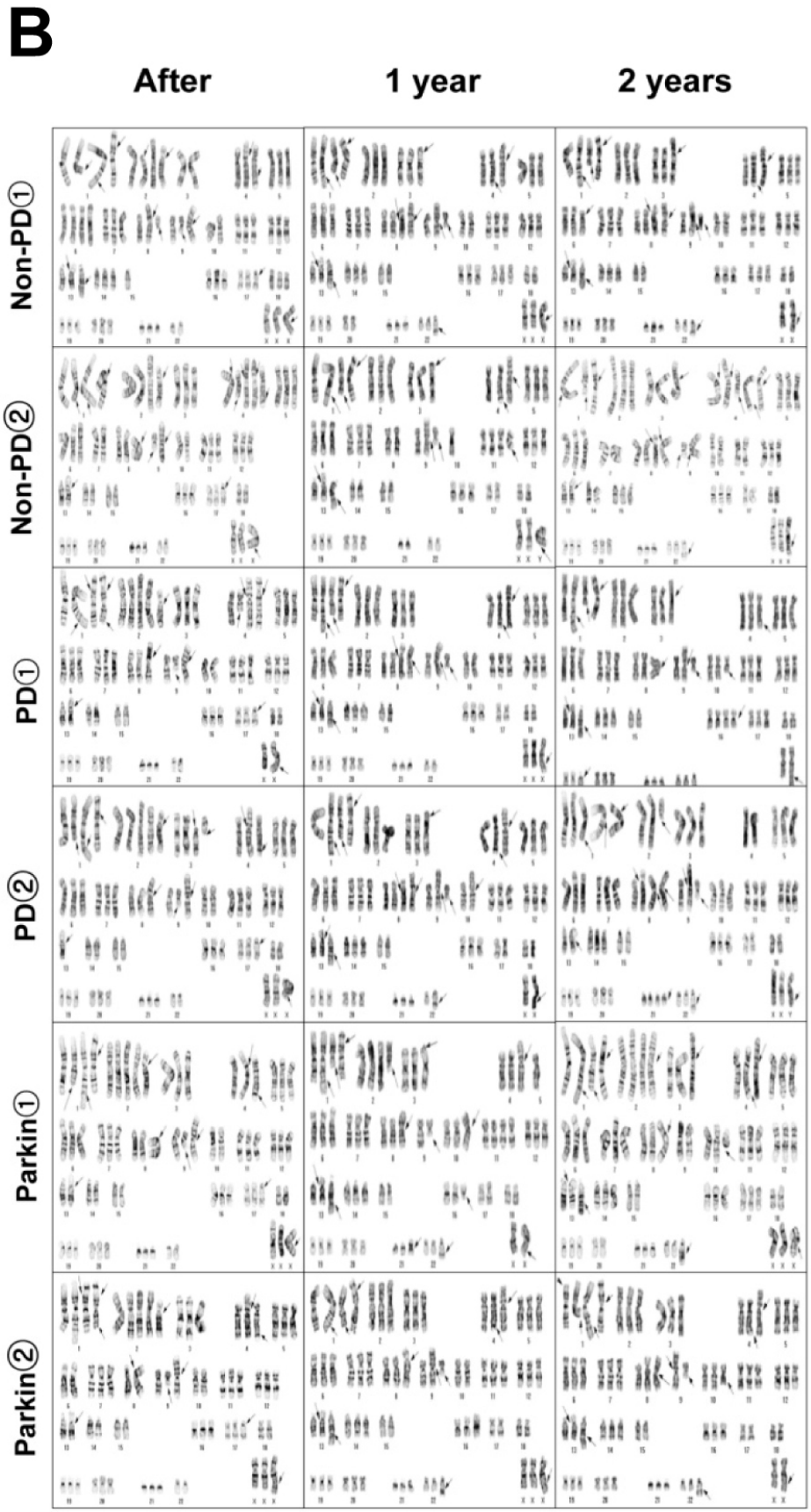

Fig. 1 (continued). (B) Karyotypic analysis of hAD-MSCs after immortalization and in the 1-year and 2-year cultures was analyzed by GTG banding. The data show the aberrant human karyotype of chromosomes in the immortalized cells. The numbers of altered chromosomes in the karyotypes of *non-PD*① were 67, 67, 67 and for *non-PD*② 65, 62, 64; those of *PD*① were 66, 66, 68 and for *PD*② 66, 65, 68; those of *Parkin*① were 66, 65, 67 and for *Parkin*② 64, 66, 65, after immortalization and in the 1-year and 2-year cultures, respectively. The arrow indicates the aberrant chromosomes in the karyotypes.

http://dx.doi.org/10.5607/en.2013.22.4.283

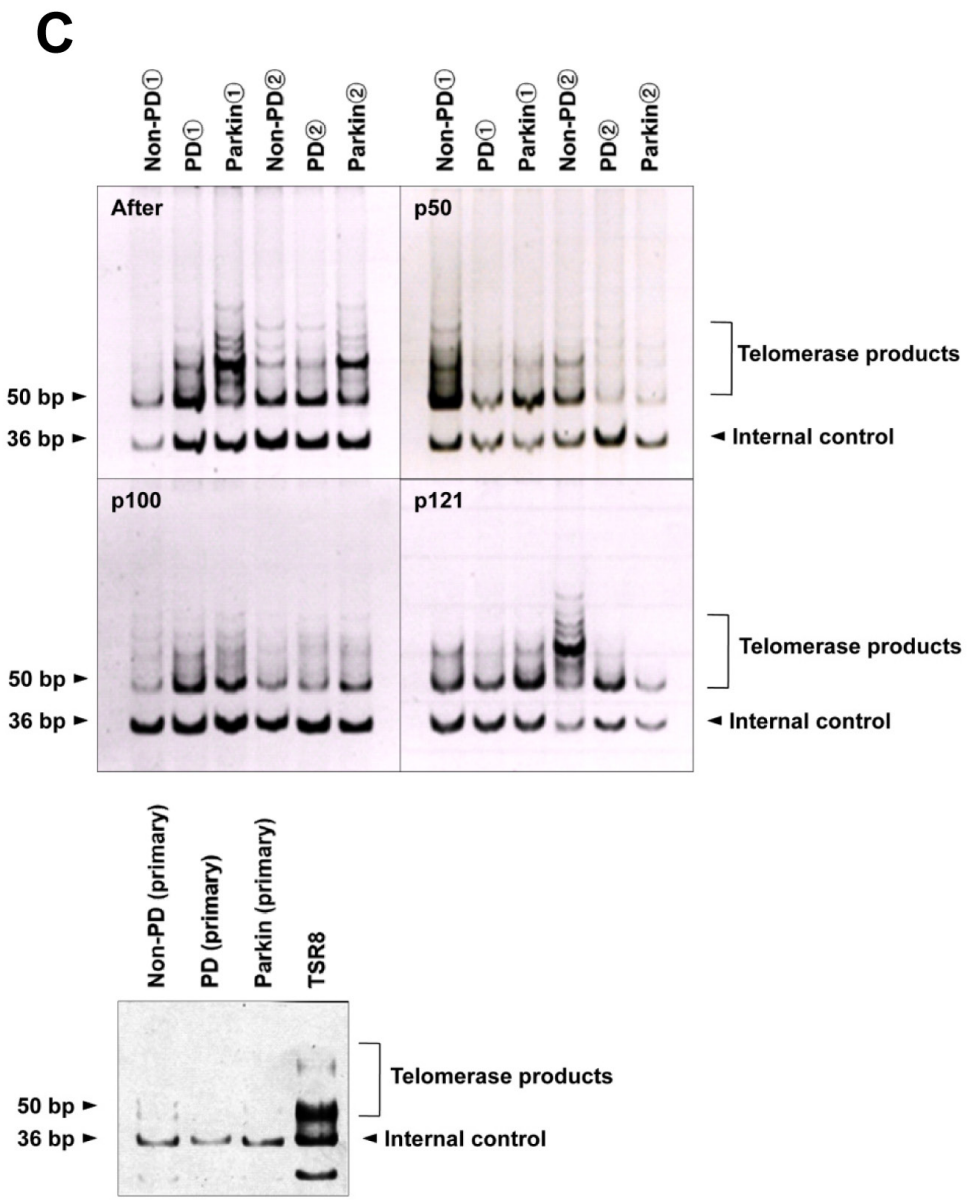

Fig. 1 (continued). (C) TRAP assay showing telomerase enzyme activity in the immortalized hAD-MSCs after immortalization, in passage 50, passage 100 and passage 121 cultures. The lanes denoted *non-PD*①, *PD*①, *Parkin*①, *non-PD*②, *PD*②, *Parkin*② represent the immortalized cells individually. The TRAP assay was performed on primary hAD-MSCs. The lanes denoted *non-PD*, *PD*, *Parkin* cells represent the primary cells individually. TSR8 was used as a positive control. A 36 bp band was used as an internal standard. The 50 bp band was the smallest telomerase product.

are expressed as the means±standard deviation (SEM). The significance of the differences between the means was determined with unpaired Student's *t*-tests and ANOVA. A difference with a p-value<0.05 was considered significant while a p-value<0.001 was considered highly significant.

RESULTS

Introduction of exogenous hTERT into normal human AD-MSCs from PD patients

To assess the utility of hTERT overexpression as a means of immortalizing adipose tissue-derived mesenchymal stromal cells, subcutaneous adipose tissues were obtained from PD patients treated with DBS surgery. The hAD-MSCs were isolated from human adult patients with early-onset hereditary familial Parkin-defect PD as well as late-onset idiopathic PD for comparison with non-PD patients with pituitary adenomas. The hAD-MSCs from patients with idiopathic PD were designated as "*PD*," from patients with Parkin-defect PD as "*Parkin*" and from patients with pituitary adenomas as "*non-PD*" for brevity. Adipose tissue was transported to the laboratory and cultured in mesenchymal stem cell expansion medium. After expanding the cells for over two

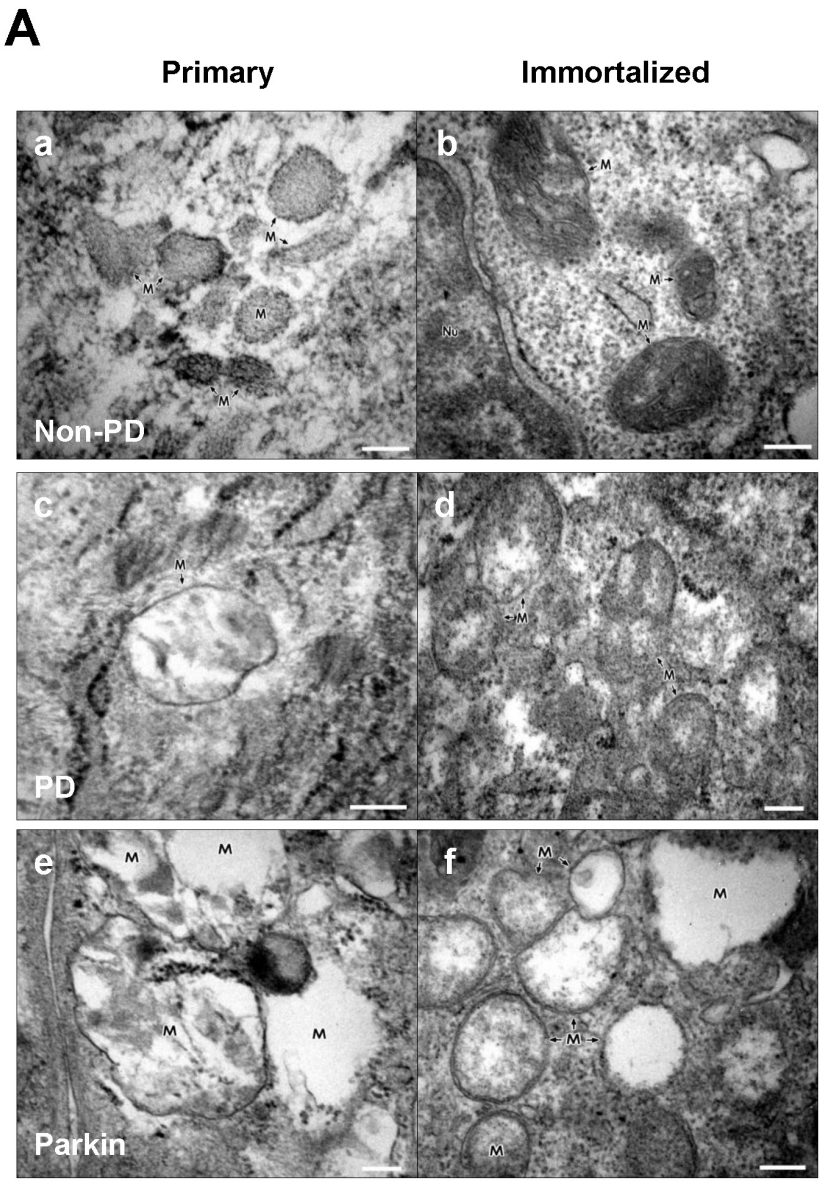

Fig. 2. Accumulation of structurally defective mitochondria in idiopathic and Parkin-defect hAD-MSCs. (A) (a) An electron micrograph showing the primary hAD-MSCs from non-PD patients. Primary cultures of non-PD were examined by electron microscopy and the mitochondria (M) are shown in the image. Note that the inner matrices of the mitochondria are generally evenly filled with cristae. Bar=200 nm. (b) An electron micrograph showing the immortalized hAD-MSCs from non-PD patients. Immortalized *non-PD* cells were examined by electron microscopy and the mitochondria (M) are shown in the image. Note that the inner mitochondrial matrices are not only evenly filled but also clearly show distinguishable cristae. Nu, nucleus. Bar=200 nm. (c) An electron micrograph showing the primary hAD-MSCs from idiopathic PD patients. Primary cultures of *PD* were examined by electron microscopy and the mitochondria (M) are shown in the image. Note that the inner mitochondrial matrices show signs of disintegration and hollow areas are visible. Bar=200 nm. (d) An electron micrograph showing the immortalized hAD-MSCs from idiopathic PD patients. Immortalized *PD* cells were examined by electron microscopy and the mitochondria (M) are shown in the image. Note that the inner mitochondrial matrices show clearly visible signs of disintegration, resulting in the many hollow areas. Bar=200 nm. (e) An electron micrograph showing the primary hAD-MSCs from PD patients with Parkin deficiency. Primary cultures of *Parkin* were examined by electron microscopy and the mitochondria (M) are shown in the image. Note that the overall shapes of the mitochondria are grossly distorted and the inner mitochondrial matrices are either severely damaged or almost absent. Bar=200 nm. (f) An electron micrograph showing the immortalized hAD-MSCs from PD patients with Parkin deficiency. Immortalized *Parkin* cells were examined by electron microscopy and the mitochondria (M) are shown in the image. Note that the inner mitochondrial matrices of many mitochondria are almost absent. Bar=200 nm. The area of the mitochondria from the electron micrograph data in the idiopathic- and Parkin-defect cells was significantly decreased by 90.3% and 90.8%, in the primary cells, and by 94.8% and 95.0% in the immortalized cells, respectively, compared to the wild type EM. The number of mitochondria from the electron micrograph data for the idiopathic- and Parkin-defect cells was significantly decreased by 94.5% and 94.7%, in the primary cells, and by 94.8% and 95.0% in the immortalized cells, respectively, compared to the wild type EM. All values are the means±SEM. ****p <0.0001.

http://dx.doi.org/10.5607/en.2013.22.4.283

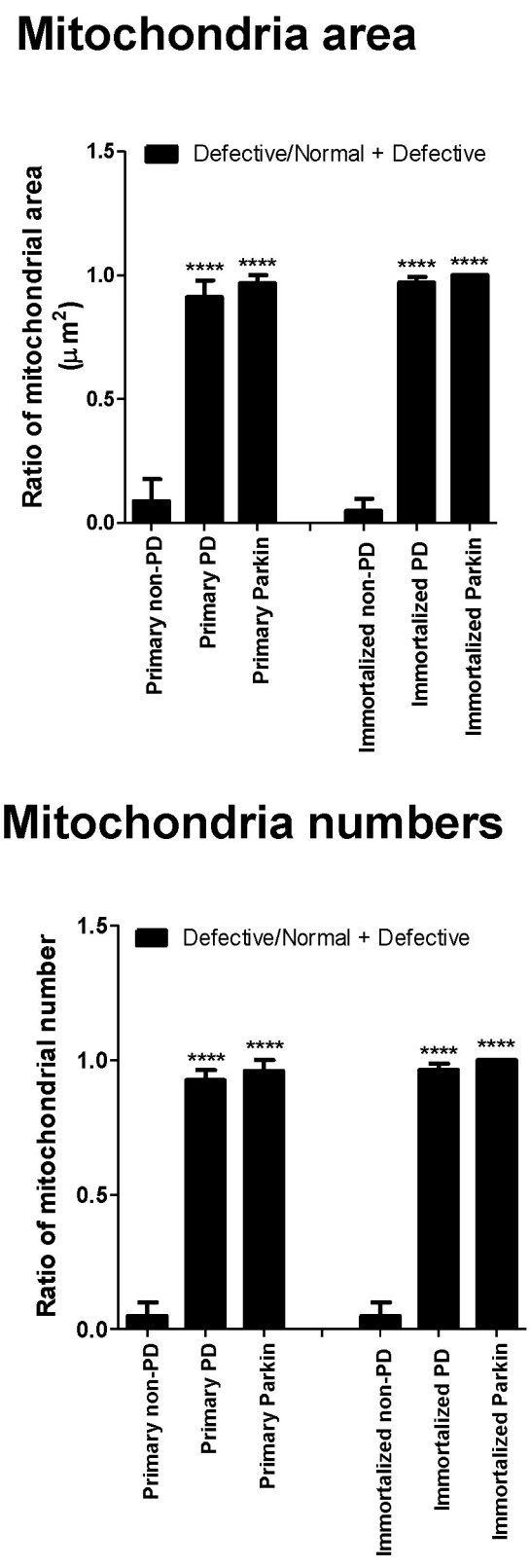

Fig. 2 (continued). (A).

weeks, homogeneous populations of hAD-MSCs were established from *non-PD*, *PD*, *Parkin* with the culture system. The cells were transduced with the pGRN145 plasmid containing the cDNA for hTERT (Fig. 1) and selection was done with media containing 30 μg/mL hygromycin-B for two to three weeks. Selected, single-cell-derived colonies for all three immortalized cells (*non-PD*, *PD*, and *Parkin*) were expanded with the concentration of hygromycin-B maintained at 10 μg/mL (Fig. 1A). The cell shapes of the selected clones belonging to the *non-PD*, *PD*, and *Parkin* cells were compared before and after immortalization, and with the six-month, one-year and two-year cultures with hTERT. To our surprise, the morphologies of the clones from the three cell lines had changed into transformed, tumorigenic cells after consistent long-term cultivation for six months, one year and two years, and those of the immortalized clones were maintained (Fig. 1A).

Extension of lifespan and changes in karyotype after immortalization accompanied by development of strong telomerase activity

There was significant induction of strong telomerase activity during the immortalization of the hAD-MSCs. Fig. 1B shows the chromosomal structures of the cells obtained immediately after the immortalization and after culturing the immortalized *non-PD*, *PD*, and *Parkin* cell lines stably for one and two years. The chromosomal structures of the primary cells before immortalization were normal and therefore not analyzed. The karyotypes of the immortal cell lines were aneuploidy with abnormal numbers of chromosomes (62~68). The telomerase activity of the cell lines was measured *in vitro* by primer extension assay in which the telomerase synthesizes telomeric repeats onto the oligonucleotide primers [27]. All chromosome numbers deviating from euploidy were aneuploidy. The analysis and nomenclature used the karyotype mark from ISCN (the International System for Human Cytogenetic Nomenclature) 2009. The results of the chromosome analysis showed that the modal numbers in the triploidy (3n) might be expressed as near-triploidy (3n±, 69±) between 58 and 80. That is, these immortalized cell lines during the two years of culturing were hypotriploidy between 58 and 68. Although the chromosome numbers of the six immortalized cell lines and two-year cultures varied between 62 and 68, the above reference supports that these are the same cell lines (Fig. 1B). Telomerase activity was identified in the extracts of the six immortal cell lines with different passages (Fig. 1C); however, the activity was not detected in the three normal somatic cell cultures (Fig. 1C). Actively proliferating normal cells did not exhibit any detectable telomerase activity in the TRAP assay. Telomerase activity was maintained for over two years in cultures

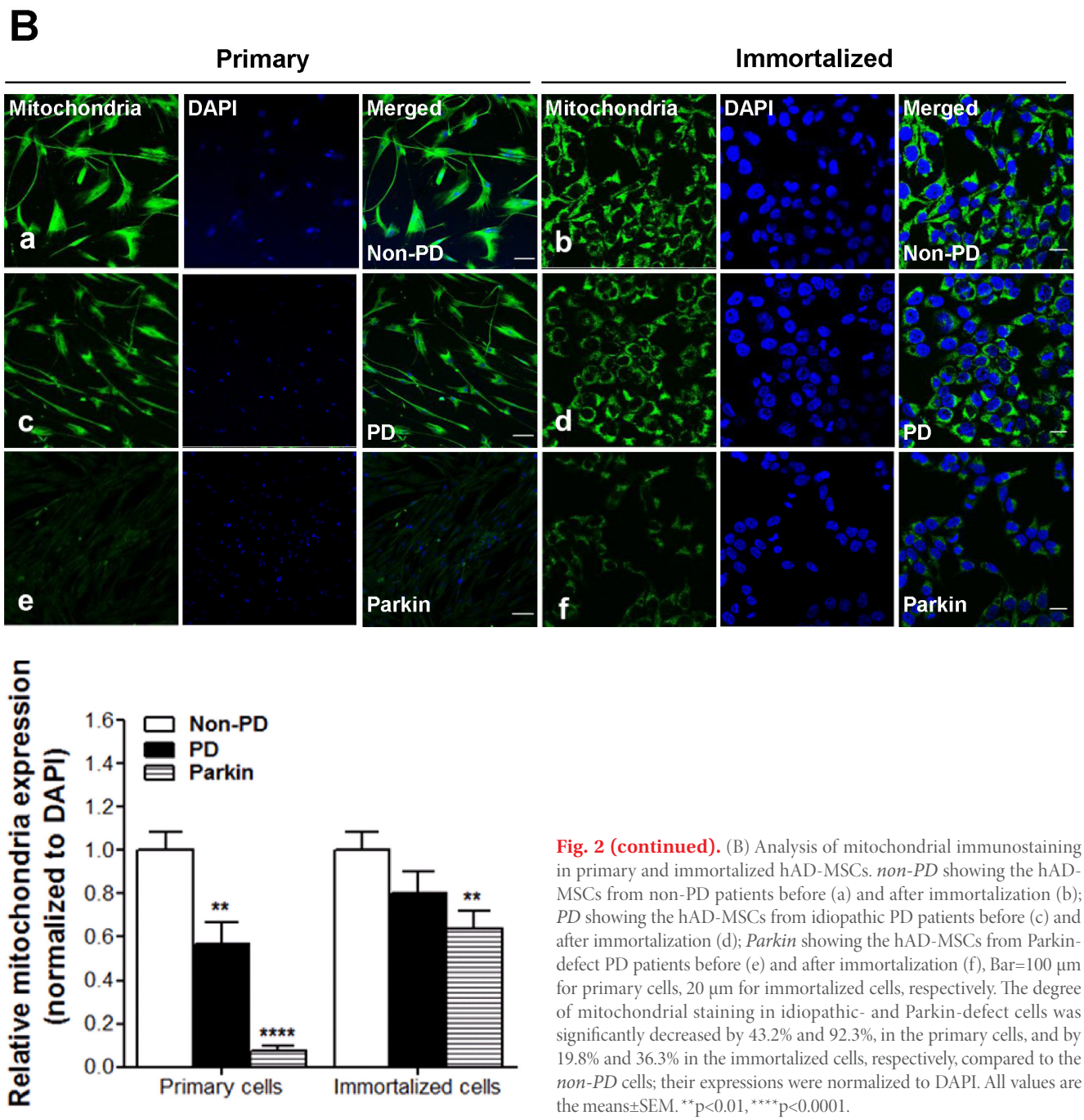

Fig. 2 (continued). (B) Analysis of mitochondrial immunostaining in primary and immortalized hAD-MSCs. *non-PD* showing the hAD-MSCs from non-PD patients before (a) and after immortalization (b); *PD* showing the hAD-MSCs from idiopathic PD patients before (c) and after immortalization (d); *Parkin* showing the hAD-MSCs from Parkin-defect PD patients before (e) and after immortalization (f), Bar=100 μm for primary cells, 20 μm for immortalized cells, respectively. The degree of mitochondrial staining in idiopathic- and Parkin-defect cells was significantly decreased by 43.2% and 92.3%, in the primary cells, and by 19.8% and 36.3% in the immortalized cells, respectively, compared to the *non-PD* cells; their expressions were normalized to DAPI. All values are the means±SEM. $^{**}p<0.01$, $^{****}p<0.0001$.

observed after immortalization and in the passages (50, 100, 121) of the immortalized cell lines. These results suggest that the telomerase activity is directly involved in telomere maintenance and in conferring cell immortality.

Distinct structural defects in the mitochondria

Mitochondrial structural defects are considered as one of underlying mechanisms associated with PD, the morphologies of the mitochondria were examined in the primary and immortalized *non-PD*, *PD*, and *Parkin* cells (Fig. 2). From the electron micrographs, the inner mitochondrial matrices of the wild type *non-PD* cells were not only evenly filled but also had clearly distinguishable cristae, while the inner mitochondrial matrices of *PD* cells had clearly visible signs of disintegration, resulting in many hollow areas; moreover, the overall shapes of the mitochondria from *Parkin* were grossly distorted and the inner mitochondrial matrices were either severely damaged or almost absent (Fig. 2A). A comparative analysis using immunofluorescent

http://dx.doi.org/10.5607/en.2013.22.4.283

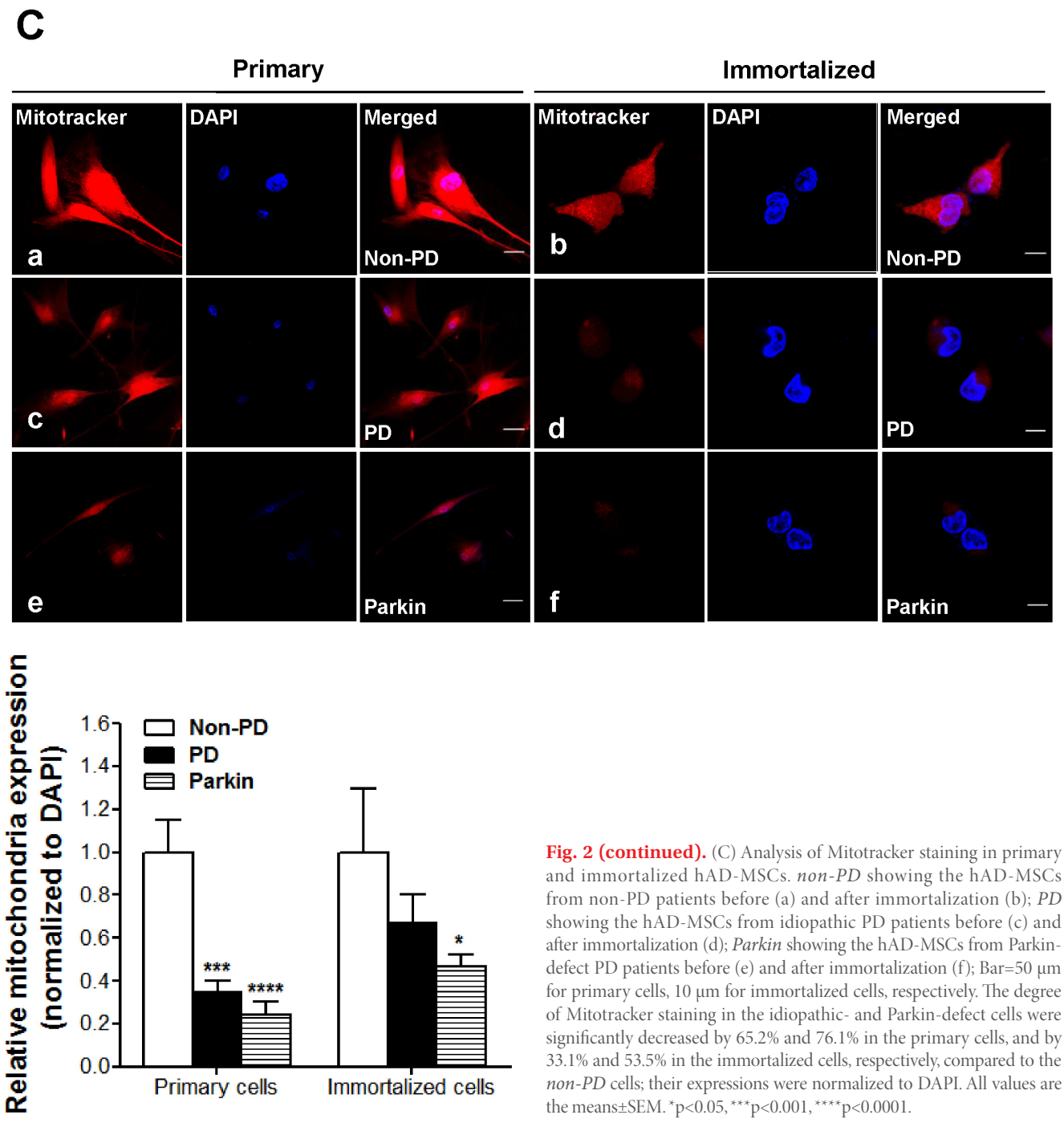

Fig. 2 (continued). (C) Analysis of Mitotracker staining in primary and immortalized hAD-MSCs. *non-PD* showing the hAD-MSCs from non-PD patients before (a) and after immortalization (b); *PD* showing the hAD-MSCs from idiopathic PD patients before (c) and after immortalization (d); *Parkin* showing the hAD-MSCs from Parkin-defect PD patients before (e) and after immortalization (f); Bar=50 μm for primary cells, 10 μm for immortalized cells, respectively. The degree of Mitotracker staining in the idiopathic- and Parkin-defect cells were significantly decreased by 65.2% and 76.1% in the primary cells, and by 33.1% and 53.5% in the immortalized cells, respectively, compared to the *non-PD* cells; their expressions were normalized to DAPI. All values are the means±SEM. *p<0.05, ***p<0.001, ****p<0.0001.

staining was done to examine mitochondria expression (Fig. 2B). The mitochondria antibody for this experiment recognized a 65 kDa nonglycosylated protein component of mitochondria found only in human cells [28]. These observations were confirmed by Mitotracker staining of defective mitochondria in the primary and immortalized idiopathic and Parkin defect cells compared to the wild type cells (Fig. 2C). The Mitotracker dyes, developed commercially by Molecular Probes (Eugene, OR), are structurally novel fluorescent probes that have been used to measure mitochondrial membrane potential, mitochondrial membrane potential-independent mitochondrial mass and photosensitization [29]. Thus, these results suggest that the mitochondria shape of the *non-PD* cells was normal; however, those of the *PD* and *Parkin* cells were damaged gradually. Whether mitochondrial damage is an important cause of PD was investigated. Particularly, the functional loss of Parkin resulted in the accumulation of

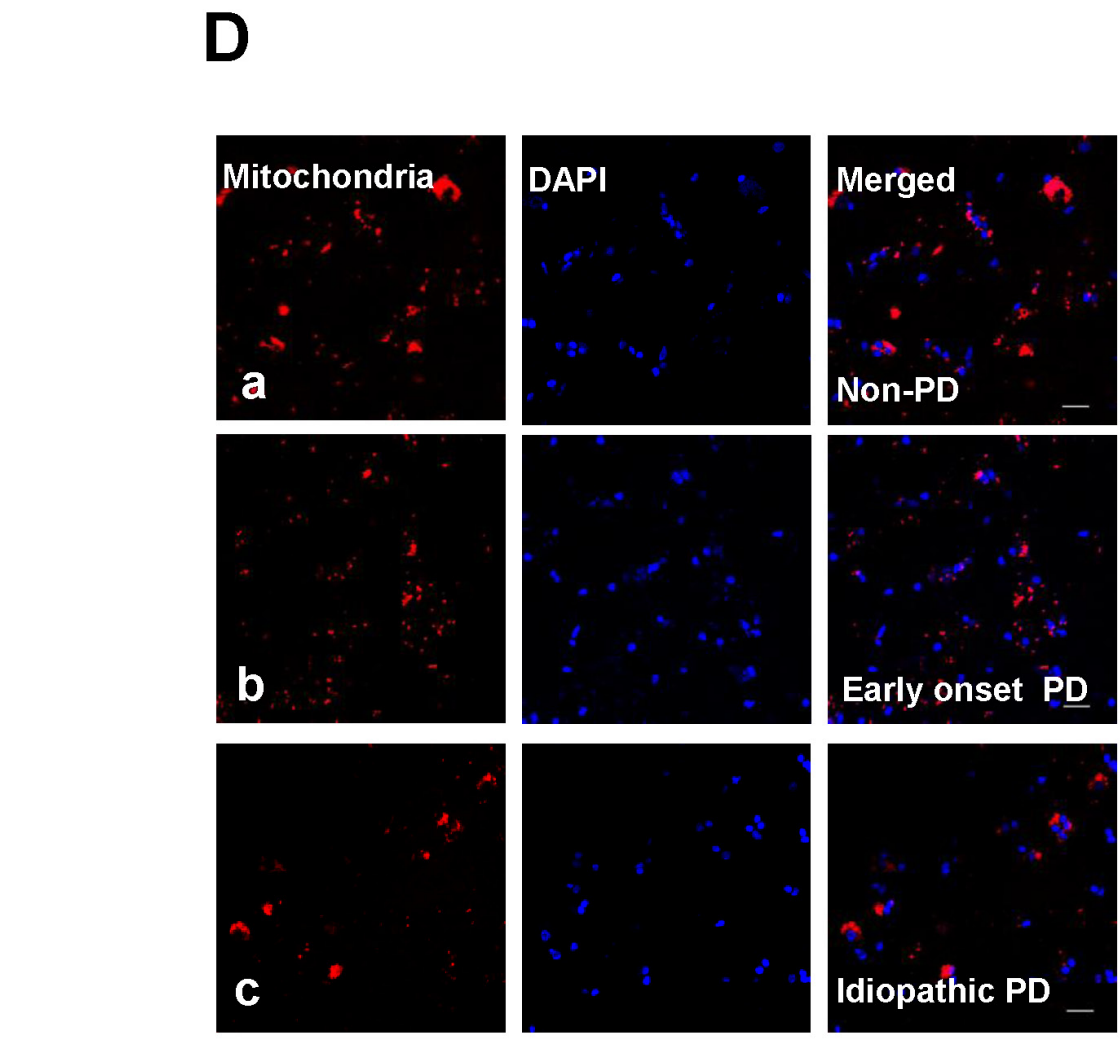

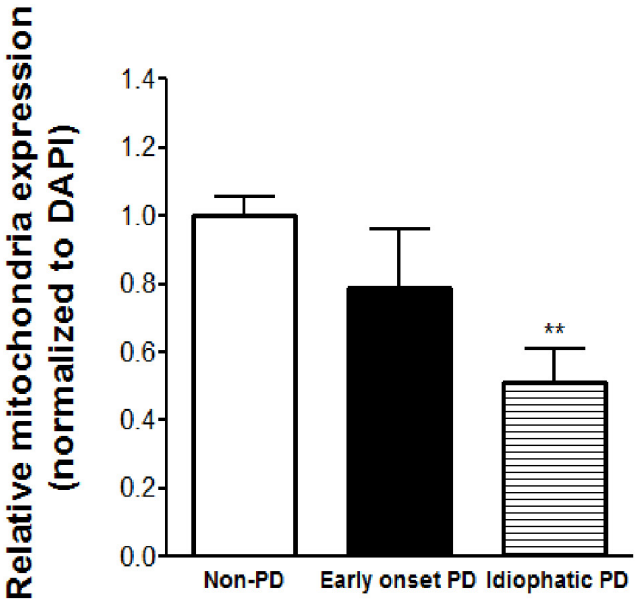

Fig. 2 (continued). (D) Analysis of mitochondrial immunofluorescence staining in brain cortex tissues from idiopathic, early onset PD and non-PD patients. The degree of mitochondrial staining in early onset and idiopathic PD tissues was significantly decreased by 21.0% and 49.0%, respectively, compared to the *non-PD* tissues; their expressions were normalized to DAPI. All values are the means±SEM. **p<0.01. Bar=20 μm.

http://dx.doi.org/10.5607/en.2013.22.4.283

structurally impaired mitochondria. Next, whether mitochondrial abnormality is also observed in the brain tissue of PD patients was investigated [30]. Brain cortex tissues of PD patients were used for mitochondrial staining to compare their morphologies with that of wild type (Fig. 2D). Particularly, mitochondrial structural defects were observed in the cortex tissues of early onset and idiopathic PD patients. The incidence rate of defective mitochondria in early onset and idiopathic tissues was significantly higher (21.0% and 49.0% ($p<0.01$) respectively) compared to that of the wild type. Thus, the functional loss of either idiopathic or early onset resulted in the accumulation of structurally impaired mitochondria.

Reduced mitochondrial complex I, II, and IV enzyme activities

Mitochondrial dysfunction is mainly characterized by the generation of reactive oxygen species (ROS), a decrease in mitochondrial complex I enzyme activity, cytochrome-c release, ATP depletion and caspase 3 activation [31]. The Parkin protein is consists of 465 amino acids with a molecular weight of 52 kDa and functions as a RING-type ubiquitin protein ligase, which possibly impairs the activity of the ubiquitin-proteosomal system and antioxidant defenses and enhances OS. Systemic mitochondrial complex I deficiency has long been implicated in the pathogenesis of idiopathic PD, which may generate additional OS in nigral neurons [32]. Here, the activity of the mitochondrial respiratory enzymes was investigated in patients with idiopathic and Parkin deficiency (Fig. 3). Both of the immortalized idiopathic and Parkin-defect cells exhibited significant reductions in the mitochondrial complex I activity by 52.7% ($p<0.0001$) and 34.9% ($p<0.001$), in complex II by 44.2% ($p<0.0001$) and 39.9% ($p<0.0001$), and in complex IV by 51.8% ($p<0.0001$) and 39.0% ($p<0.001$), respectively, compared to the wild type cells (Fig. 3A). The immortalized idiopathic cells had greater reductions in the mitochondrial complex I, II, and IV activities than that of the Parkin-defect cells. The expression level of proteins for the mitochondrial preparations of the immortalized cells were normalized with the mitochondrial marker prohibitin, not with the cytosolic marker actin (Fig. 3B).

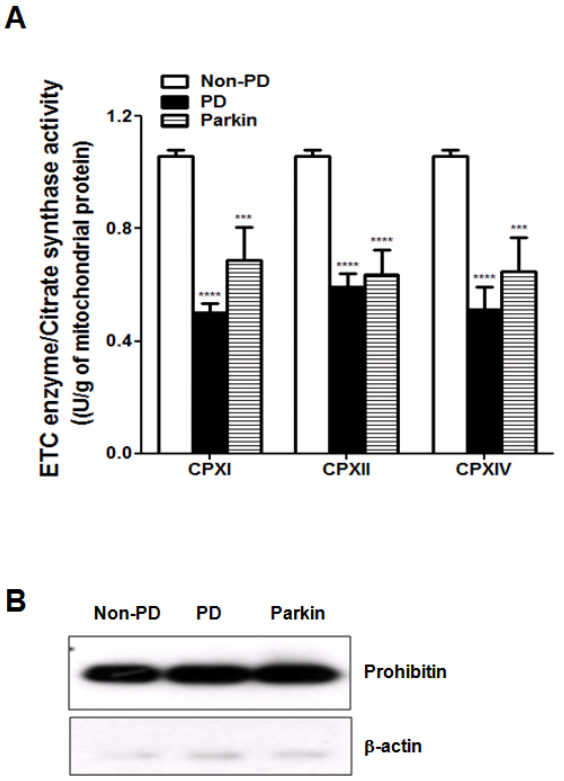

Fig. 3. Reduction in the mitochondria complex I, II, and IV activities in idiopathic and Parkin-defect immortalized hAD-MSCs. (A) The activities of ETC enzymes (complex I, II, and IV) and citrate synthase were measured in mitochondria isolated from the immortalized non-PD, idiopathic and Parkin-defect cells. Compared to wild type cells, idiopathic cells showed significant decreases in mitochondria complex I, II, and IV activities by 52.7%, 44.2%, and 51.8%, respectively. Moreover, Parkin-defect cells showed decreases by 34.9%, 39.9%, and 39.0% in mitochondria complex I, II, and IV activities, respectively. All values are the means±SEM from three independent experiments. ****$p<0.0001$, ***$p<0.001$, CPXI (NADH dehydrogenase), CPXII (Succinate dehydrogenase), CPXIV (Cytochrome c oxidase). (B) Western blot analysis of prohibitin expression in mitochondria isolated from the immortalized wild type, idiopathic and Parkin-defect cells.

Altered expression of PD specific marker proteins

After investigating the key roles of mitochondrial dysfunction in PD pathogenesis in the established wild type, idiopathic and Parkin-defect mesenchymal stromal cells isolated from the adipose tissues of PD patients, comparative Western blot analyses were first performed to identify the expression of specific marker proteins (Fig. 4). There was a slight increase in a mitochondrial chaperone heat shock protein 60 (HSP60) in the immortalized cells (Fig. 4A). In addition, the altered expression of a molecular chaperone heat shock protein 90 (HSP90) was observed in the immortalized cells (Fig. 4B). Moreover, cytochrome b5, a ubiquitous electron transport hemoprotein, and GRP78, a central regulator of endoplasmic reticulum homeostasis, showed a slight increase in the mitochondrial fraction of the idiopathic and Parkin-defect immortalized cells (Fig. 4C). The expression level of proteins for the mitochondrial preparations of the immortalized cells were normalized with the mitochondrial marker prohibitin, not with the cytosolic marker actin (Fig. 4C).

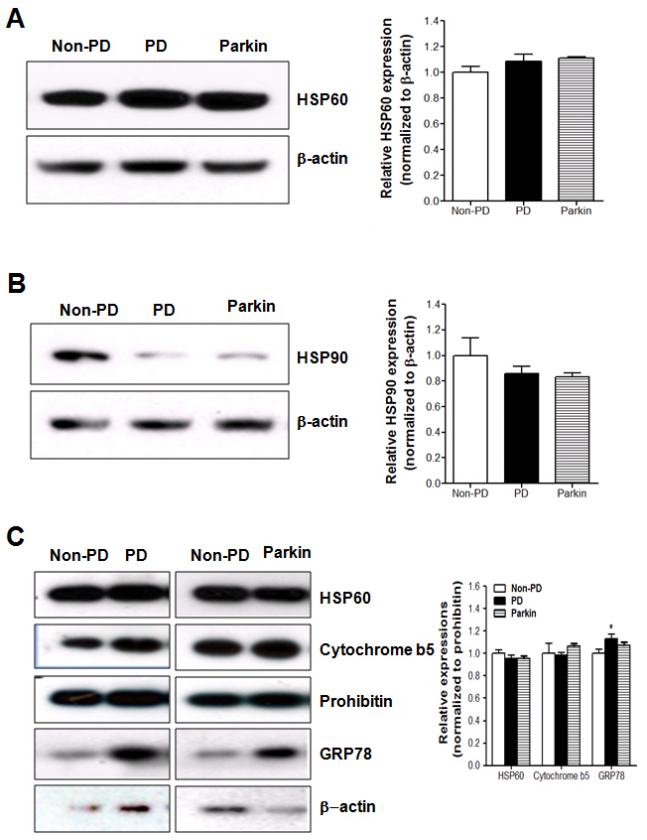

Fig. 4. Altered expressions of PD specific marker proteins in idiopathic and Parkin-defect immortalized hAD-MSCs. (A) The levels of HSP60 in the total cell lysates of the immortalized idiopathic and Parkin-defect cells, compared to the wild type cells, were assessed by Western blot analysis. From the quantitative analysis, the relative expression of HSP60 protein was determined. All values are the means±SEM. (B) The levels of HSP90 in the total cell lysates of the immortalized idiopathic and Parkin-defect cells, compared to the wild type cells, were assessed by Western blot analysis. From the quantitative analysis, the relative expression of HSP90 protein was determined. All values are the means±SEM. (C) The levels of HSP60, Cytochrome b5, prohibitin, β-actin, GRP78 in the mitochondrial fractions of the immortalized idiopathic and Parkin-defect cells, compared to wild type cells, were assessed by Western blot analysis. From the quantitative analysis, the relative expressions of HSP60, Cytochrome b5 and GRP78 proteins were determined. All values are the means±SEM. *$p<0.05$.

DISCUSSION

Defective mitochondrial function and increased OS are known to have key roles in the pathogenesis of PD, which contribute to the selective loss of dopaminergic neurons in PD. Mitochondrial abnormalities have mainly been reported in various non-dopaminergic cells and tissue samples from human patients as well as transgenic mouse and fruit fly models of PD [4, 6]. Thus, mitochondria represent a promising target for the development of PD biomarkers. Biochemical detection methods for potential biomarkers of PD include genetic screening, mitochondrial complex I measurements, and α-synuclein levels and its isoforms in the blood [2, 3]. However, the limited availability of dopaminergic cell lines has prevented investigation of mitochondrial abnormalities in PD. For the first time, we have established hTERT-immortalized wild type, idiopathic and Parkin-defect MSCs isolated from the adipose tissues of PD patients. In order to overcome the cellular senescence of primary cultured hAD-MSCs of PD patients, the wild type, idiopathic and Parkin-defect MSCs were isolated from the adipose tissues of PD patients which were immortalized by hTERT. These hTERT-immortalized hAD-MSC cell lines established from patients with idiopathic and familial Parkin-defect PD had different activities in mitochondria function and in the morphologies of their structures, which could help in understanding better the pathogenesis of PD. Finally, these hTERT-immortalized hAD-MSC cell lines described in this study had altered PD specific markers, which could contribute to the development of early diagnostic markers and effective therapy targets for PD. One possible concern is that we used the control patients with pituitary adenomas. However, we may not consider that the adipose tissue taken from the abdominal sites of patients with pituitary adenomas had the characteristics of a tumor linked to mitochondrial changes. We usually collected normal adipose tissues from the patients to reconstruct the sellar floor after transsphenoidal adenomectomy. Therefore, we might suppose that the abdominal adipose tissue-derived mesenchymal cells of two patients with pituitary adenomas were normal cells.

Exogenous hTERT expression has been shown to extend both safely and effectively cellular lifespan and remove senescence as a major obstacle in tissue engineering and cell based therapies [33]. Unexpectedly, we produced transformed immortalized cell lines with a chromosome abnormality. The karyotypes of these immortal cell lines were determined as aneuploidy with abnormal numbers of chromosomes ranging between 62~68. An extra or missing chromosome is a common cause of genetic disorders. Some cancer cells generally have abnormal numbers of chromosomes. According to the chromosomal numbers after culturing the six immortalized cell lines for one and two years, the structural phenotypes were similar with the only in difference being in the chromosomal numbers such as 3n=69. Therefore, we suggest that these one- and two-year cultures are the same immortalized cell lines with both cell lines having their variation in chromosomal numbers confirmed. Okubo et al. showed in detail that a change in the karyotypes of human B-lymphoblastoid cell lines transformed by Epstein-Barr virus during the process of immortalization was correlated to the development of telomerase activity using eight immortalized cell lines [34]. It remains to be

http://dx.doi.org/10.5607/en.2013.22.4.283

elucidated whether the chromosomal rearrangement is the cause of the immortalization accompanied by the strong telomerase activity or is a result of the immortalization process [34]. Moreover, Belgiovine et al. [35] reviewed telomerase immortalization of somatic cells and its consequences and examined the complex role of telomerase in tumorigenesis. Cell lines with neoplastic transformation of telomerase expression can be useful models for studying molecular changes in human carcinogenesis.

There could be a possible correlation between chromosomal instability and the hTERT activity of the cell lines in this study. In the literature, there have been several reports on chromosomal instability driven by the hTERT activity. Fauth et al. [36] immortalized a panel of normal mammary fibroblasts and endothelial cells with the catalytic subunit of telomerase (hTERT) and a temperature-sensitive mutant of the SV40 large-tumor (tsLT) oncoprotein in different orders in early- and late-passage stocks. They maintained the immortalized cell lines in continuous culture for up to 90 passages, equivalent to >300 population doublings (PDs) post-explantation during 3 years of continuous propagation. They karyotyped the cultures at different passages. The cultures that received hTERT first followed by tsLT maintained a near-diploid karyotype for more than 150 PDs. However, in late-passage stocks (>200 PDs), the metaphase cells were mostly aneuploid. In contrast, the reverse order of gene transduction resulted in a marked early aneuploidy and chromosomal instability, already visible after 50 PDs. Tsuruga et al. [37] established two immortalized hepatocyte lines called HHE6E7T-1 and HHE6E7T-2 from human adult hepatocytes by introducing HPV16 E6/E7 and hTERT. Karyotype analysis showed that the HHE6E7T-1 cells remained near diploid but the HHE6E7T-2 cells showed severe aneuploidy at 150 PDs. Wen et al. [38] reported on the telomere-driven karyotypic complexity with p16INK4a inactivation in TP53-competent immortalized bone marrow endothelial cells by hTERT transduction. They showed a specific association between the p16INK4 inactivation and the evolution of karyotypic complexity in the TP53-competent cells. These results show that complex karyotypes can evolve in TP53-competent cells and provide evidence that p16INK4a functions as a gatekeeper to prevent telomere-driven cytogenetic evolution.

Although these immortalized cells had chromosomal aberrations, the telomerase activity was identified in six immortal cell lines over two years and in different passages in the extracts of human cells; however, three pre-immortal cell lines showed no telomerase activity and had normal diploid karyotypes. These methods were used to measure the telomerase activity in dividing cultures of various immortal cell lines and normal somatic cells derived from human adipose tissues. These results suggest that the telomerase activity is involved in telomerase maintenance, linking this enzyme to cell immortality. In this study, hAD-MSCs had mostly normal diploid karyotypes before immortalization; however, all had abnormal karyotypes after immortalization accompanied by strong telomerase activity. The pre- and post-immortalization of hAD-MSCs will be an effective system to study the mechanisms of not only the immortalization of hAD-MSCs, but also PD. These immortalized hAD-MSC cell lines established from patients with idiopathic and familial Parkin-defect PD while artificial could be used as a good cellular model to evaluate mitochondrial dysfunction in the pathogenesis of PD.

Previously, we investigated selective gene expression profiles derived from primary cultured AD-MSCs from PD patients with Parkin-defect PD as well as idiopathic PD using transcriptome cDNA microarray analysis [23]. Our data was only preliminary; however, high throughput microarray screening using these cell lines has identified functional groups of genes affected by mitochondria dysfunction and OS. We analyzed PD-related differentially regulated genes by OS in *non-PD*, *PD* and *Parkin* cells [23]. Eight groups of genes were categorized as oxido-reductase, endoplasmic reticulum/ubiquitin-like, exocytosis/membrane trafficking, apoptosis/cell survival, structure/transport, translation, nuclear/transcriptional, and cell cycle genes. Linearly increased sequences of genes in all groups could be explained by the increased compensation of vulnerability caused by OS. Furthermore, for the first time, we produced hTERT-immortalized wild type, idiopathic and Parkin-defect MSCs isolated from the adipose tissues of PD patients to investigate PD specific mitochondria dysfunction in models of idiopathic and familial PD. These immortalized cell lines allowed us to analyze mitochondrial dysfunction at the molecular level. Our immortalized idiopathic and Parkin-defect AD-MSCs exhibited significant mitochondrial pathophenotypes such as OS, dramatically decreased mitochondrial complex I, II and IV activities, severe loss of mitochondrial cristae and abnormal mitochondrial morphologies.

Heat shock proteins (HSPs or molecular chaperones) can either aid in the folding and maintenance of newly translated proteins or lead to the degradation of misfolded and destabilized proteins [39]. HSPs are particularly important in PD because aberrant protein aggregation and neuron degeneration are common pathophysiologies of PD. HSPs have two main cellular functions. One is to promote the function of the ubiquitin-proteasome system (UPS) and the other is to inhibit apoptotic activity in PD [39]. HSP60 is a mitochondrial chaperone that is constitutively expressed in the mitochondrial matrix. It functions to catalyze the proper folding and assemble of proteins imported into the mitochondria and to correct mis-folded proteins that have been

damaged by OS [40]. HSP90 has been recently identified as the predominant chaperone implicated in α-synuclein (AS)-evoked pathologies [41]. Uryu et al. [41] showed that HSP90 together with ubiquitin massively co-localizes *in vivo* with soluble AS as well as with amyloid filaments, suggesting a possible role of HSP90 in modulating the folding and suppression of incorrectly folded AS. The levels of HSP60 in the cell extracts of the immortalized cells showed a slight increase and that of HSP90 in the immortalized cells was decreased in both the idiopathic and Parkin-defect cells.

Cytochrome b5 functions as an electron transfer component in a number of oxidation reactions [42]. Increased cytochrome b5 levels in idiopathic and Parkin-defect cells may be because of compensatory mechanisms in response to the defective electron flows from ETC enzyme dysfunction. Specifically, increased cytochrome b5 may help to facilitate electron transfer from NADH to cytochrome c [43]. The ER stress response, also termed the unfolded protein response (UPR), serves to protect cells against the toxic build-up of un-/mis-folded proteins. The first step in UPR is the recognition of unfolded proteins by the HSP70-class chaperone glucose regulated protein 78, also known as BiP (GRP78/BiP). Recently, Gorbatyuk et al. suggested that the molecular chaperone GRP78/BiP plays a neuroprotective role in α-synuclein-induced Parkinson-like neurodegeneration [44]. Our data showed increased levels of GRP78 in the idiopathic and Parkin-deficient cells, which possibly could also explain the compensatory mechanisms.

In conclusion, for the first time, we have established hTERT-immortalized wild type, idiopathic and Parkin-defect mesenchymal stromal cells isolated from the adipose tissues of patients. We have showed that the hTERT-immortalized hAD-MSC cell lines established from patients with idiopathic and familial Parkin-defect PD could be used as good cellular models to evaluate mitochondrial dysfunction to understand better the pathogenesis of PD and to develop early diagnostic markers and effective therapy targets for PD. Noticeably, PD-specific mitochondrial dysfunction included reduced complex I, II, and IV enzyme activities, abolished cristae and accumulated mitochondria that were damaged. The OS-induced pathological signaling involves the altered expressions of PD specific markers. Further functional characterization of mitochondria DNA and whole genome sequencing analysis may help to explain the complex pathogenesis of PD in dopamine neurons and in the development of novel therapeutic agents for PD.

ACKNOWLEDGEMENTS

The authors would like to thank the patients and their relatives for their participation. This study was supported by a grant from the Korea Institute of Planning & Evaluation for Technology in Food, Agriculture, Forestry, and Fisheries, Republic of Korea (311011-05-3-SB020) and from the Korea Healthcare Technology R&D Project, Ministry of Health & Welfare, Republic of Korea (HI09C13540100, HI12C02050101).

REFERENCES

1. Hoepken HH, Gispert S, Azizov M, Klinkenberg M, Ricciardi F, Kurz A, Morales-Gordo B, Bonin M, Riess O, Gasser T, Kögel D, Steinmetz H, Auburger G (2008) Parkinson patient fibroblasts show increased alpha-synuclein expression. Exp Neurol 212:307-313.
2. Henchcliffe C, Beal MF (2008) Mitochondrial biology and oxidative stress in Parkinson disease pathogenesis. Nat Clin Pract Neurol 4:600-609.
3. Abou-Sleiman PM, Muqit MM, Wood NW (2006) Expanding insights of mitochondrial dysfunction in Parkinson's disease. Nat Rev Neurosci 7:207-219.
4. Shim JH, Yoon SH, Kim KH, Han JY, Ha JY, Hyun DH, Paek SH, Kang UJ, Zhuang X, Son JH (2011) The antioxidant Trolox helps recovery from the familial Parkinson's disease-specific mitochondrial deficits caused by PINK1- and DJ-1-deficiency in dopaminergic neuronal cells. Mitochondrion 11:707-715.
5. Palacino JJ, Sagi D, Goldberg MS, Krauss S, Motz C, Wacker M, Klose J, Shen J (2004) Mitochondrial dysfunction and oxidative damage in parkin-deficient mice. J Biol Chem 279:18614-18622.
6. Greene JC, Whitworth AJ, Kuo I, Andrews LA, Feany MB, Pallanck LJ (2003) Mitochondrial pathology and apoptotic muscle degeneration in Drosophila parkin mutants. Proc Natl Acad Sci U S A 100:4078-4083.
7. Yoo MS, Kawamata H, Kim DJ, Chun HS, Son JH (2004) Experimental strategy to identify genes susceptible to oxidative stress in nigral dopaminergic neurons. Neurochem Res 29:1223-1234.
8. Dexter DT, Wells FR, Lees AJ, Agid F, Agid Y, Jenner P, Marsden CD (1989) Increased nigral iron content and alterations in other metal ions occurring in brain in Parkinson's disease. J Neurochem 52:1830-1836.
9. Sriram K, Pai KS, Boyd MR, Ravindranath V (1997) Evidence for generation of oxidative stress in brain by MPTP: in vitro and in vivo studies in mice. Brain Res 749:44-52.
10. Engelhardt JF (1999) Redox-mediated gene therapies for environmental injury: approaches and concepts. Antioxid

http://dx.doi.org/10.5607/en.2013.22.4.283

Redox Signal 1:5-27.
11. Kuan CY, Burke RE (2005) Targeting the JNK signaling pathway for stroke and Parkinson's diseases therapy. Curr Drug Targets CNS Neurol Disord 4:63-67.
12. Miller RM, Federoff HJ (2005) Altered gene expression profiles reveal similarities and differences between Parkinson disease and model systems. Neuroscientist 11:539-549.
13. Peng J, Mao XO, Stevenson FF, Hsu M, Andersen JK (2004) The herbicide paraquat induces dopaminergic nigral apoptosis through sustained activation of the JNK pathway. J Biol Chem 279:32626-32632.
14. Stefanis L, Larsen KE, Rideout HJ, Sulzer D, Greene LA (2001) Expression of A53T mutant but not wild-type alpha-synuclein in PC12 cells induces alterations of the ubiquitin-dependent degradation system, loss of dopamine release, and autophagic cell death. J Neurosci 21:9549-9560.
15. Anglade P, Vyas S, Javoy-Agid F, Herrero MT, Michel PP, Marquez J, Mouatt-Prigent A, Ruberg M, Hirsch EC, Agid Y (1997) Apoptosis and autophagy in nigral neurons of patients with Parkinson's disease. Histol Histopathol 12:25-31.
16. Choi KC, Kim SH, Ha JY, Kim ST, Son JH (2010) A novel mTOR activating protein protects dopamine neurons against oxidative stress by repressing autophagy related cell death. J Neurochem 112:366-376.
17. Pittenger MF, Mackay AM, Beck SC, Jaiswal RK, Douglas R, Mosca JD, Moorman MA, Simonetti DW, Craig S, Marshak DR (1999) Multilineage potential of adult human mesenchymal stem cells. Science 284:143-147.
18. Zuk PA, Zhu M, Ashjian P, De Ugarte DA, Huang JI, Mizuno H, Alfonso ZC, Fraser JK, Benhaim P, Hedrick MH (2002) Human adipose tissue is a source of multipotent stem cells. Mol Biol Cell 13:4279-4295.
19. Hahn WC, Stewart SA, Brooks MW, York SG, Eaton E, Kurachi A, Beijersbergen RL, Knoll JH, Meyerson M, Weinberg RA (1999) Inhibition of telomerase limits the growth of human cancer cells. Nat Med 5:1164-1170.
20. Blackburn EH (1991) Structure and function of telomeres. Nature 350:569-573.
21. Morin GB (1989) The human telomere terminal transferase enzyme is a ribonucleoprotein that synthesizes TTAGGG repeats. Cell 59:521-529.
22. Bodnar AG, Ouellette M, Frolkis M, Holt SE, Chiu CP, Morin GB, Harley CB, Shay JW, Lichtsteiner S, Wright WE (1998) Extension of life-span by introduction of telomerase into normal human cells. Science 279:349-352.
23. Moon HE, Park HW, Shin HY, Paek SL, Kim DG, Son JH, Paek SH (2010) Genetic profiling in human adipose tissue-derived mesenchymal stromal cells from the idiopathic and familial parkin-deficient patients of Parkinson's disease in comparison with non-PD patients. Tissue Eng Regen Med 7:237-247.
24. Janssen AJ, Trijbels FJ, Sengers RC, Smeitink JA, van den Heuvel LP, Wintjes LT, Stoltenborg-Hogenkamp BJ, Rodenburg RJ (2007) Spectrophotometric assay for complex I of the respiratory chain in tissue samples and cultured fibroblasts. Clin Chem 53:729-734.
25. Cooperstein SJ, Lazarow A (1951) A microspectrophotometric method for the determination of cytochrome oxidase. J Biol Chem 189:665-670.
26. Sugden PH, Newsholme EA (1975) Activities of citrate synthase, NAD+-linked and NADP+-linked isocitrate dehydrogenases, glutamate dehydrogenase, aspartate aminotransferase and alanine aminotransferase in nervous tissues from vertebrates and invertebrates. Biochem J 150:105-111.
27. Greider CW, Blackburn EH (1985) Identification of a specific telomere terminal transferase activity in Tetrahymena extracts. Cell 43:405-413.
28. Kehat I, Khimovich L, Caspi O, Gepstein A, Shofti R, Arbel G, Huber I, Satin J, Itskovitz-Eldor J, Gepstein L (2004) Electromechanical integration of cardiomyocytes derived from human embryonic stem cells. Nat Biotechnol 22:1282-1289.
29. Buckman JF, Hernández H, Kress GJ, Votyakova TV, Pal S, Reynolds IJ (2001) MitoTracker labeling in primary neuronal and astrocytic cultures: influence of mitochondrial membrane potential and oxidants. J Neurosci Methods 104:165-176.
30. Ravid R, Ferrer I (2012) Brain banks as key part of biochemical and molecular studies on cerebral cortex involvement in Parkinson's disease. FEBS J 279:1167-1176.
31. Schapira AH (2012) Targeting mitochondria for neuroprotection in Parkinson's disease. Antioxid Redox Signal 16:965-973.
32. Müftüoglu M, Elibol B, Dalmizrak O, Ercan A, Kulaksiz G, Ogüs H, Dalkara T, Ozer N (2004) Mitochondrial complex I and IV activities in leukocytes from patients with parkin mutations. Mov Disord 19:544-548.
33. Lee KM, Choi KH, Ouellette MM (2004) Use of exogenous hTERT to immortalize primary human cells. Cytotechnology 45:33-38.
34. Okubo M, Tsurukubo Y, Higaki T, Kawabe T, Goto M, Murase T, Ide T, Furuichi Y, Sugimoto M (2001) Clonal chromosomal aberrations accompanied by strong telomerase activity in

immortalization of human B-lymphoblastoid cell lines transformed by Epstein-Barr virus. Cancer Genet Cytogenet 129:30-34.

35. Belgiovine C, Chiodi I, Mondello C (2008) Telomerase: cellular immortalization and neoplastic transformation. Multiple functions of a multifaceted complex. Cytogenet Genome Res 122:255-262.
36. Fauth C, O'Hare MJ, Lederer G, Jat PS, Speicher MR (2004) Order of genetic events is critical determinant of aberrations in chromosome count and structure. Genes Chromosomes Cancer 40:298-306.
37. Tsuruga Y, Kiyono T, Matsushita M, Takahashi T, Kasai H, Matsumoto S, Todo S (2008) Establishment of immortalized human hepatocytes by introduction of HPV16 E6/E7 and hTERT as cell sources for liver cell-based therapy. Cell Transplant 17:1083-1094.
38. Wen VW, Wu K, Baksh S, Hinshelwood RA, Lock RB, Clark SJ, Moore MA, Mackenzie KL (2006) Telomere-driven karyotypic complexity concurs with p16INK4a inactivation in TP53-competent immortal endothelial cells. Cancer Res 66:10691-10700.
39. Luo GR, Chen S, Le WD (2007) Are heat shock proteins therapeutic target for Parkinson's disease? Int J Biol Sci 3:20-26.
40. Martin J (1997) Molecular chaperones and mitochondrial protein folding. J Bioenerg Biomembr 29:35-43.
41. Uryu K, Richter-Landsberg C, Welch W, Sun E, Goldbaum O, Norris EH, Pham CT, Yazawa I, Hilburger K, Micsenyi M, Giasson BI, Bonini NM, Lee VM, Trojanowski JQ (2006) Convergence of heat shock protein 90 with ubiquitin in filamentous alpha-synuclein inclusions of alpha-synucleinopathies. Am J Pathol 168:947-961.
42. Schenkman JB, Jansson I (2003) The many roles of cytochrome b5. Pharmacol Ther 97:139-152.
43. Strittmatter CF, Ball EG (1952) A hemochromogen component of liver microsomes. Proc Natl Acad Sci U S A 38:19-25.
44. Gorbatyuk MS, Shabashvili A, Chen W, Meyers C, Sullivan LF, Salganik M, Lin JH, Lewin AS, Muzyczka N, Gorbatyuk OS (2012) Glucose regulated protein 78 diminishes α-synuclein neurotoxicity in a rat model of Parkinson disease. Mol Ther 20:1327-1337.

 http://dx.doi.org/10.5607/en.2013.22.4.283